The Spine Journal 19 (2019) 1264–1275

Basic Science

Discriminating spatiotemporal movement strategies during spine flexion-extension in healthy individuals

Shawn M. Beaudette, PhD[a], Derek P. Zwambag, PhD[b], Ryan B. Graham, PhD[a], Stephen H.M. Brown, PhD[c,*]

[a] *School of Human Kinetics, Faculty of Health Sciences, University of Ottawa, Ottawa Ontario, Canada*
[b] *Department of Kinesiology and Physical Education, Wilfrid Laurier University, Waterloo Ontario, Canada*
[c] *Department of Human Health and Nutritional Sciences, University of Guelph, Guelph Ontario, Canada*

Received 23 October 2018; revised 4 February 2019; accepted 5 February 2019

ABSTRACT

BACKGROUND CONTEXT: The spine is an anatomically complex system with numerous degrees of freedom. Due to this anatomical complexity, it is likely that multiple motor control options exist to complete a given task.

PURPOSE: To identify if distinct spine spatiotemporal movement strategies are utilized in a homogenous sample of young healthy participants.

STUDY DESIGN: Kinematic data were captured from a single cohort of male participants (N=51) during a simple, self-controlled spine flexion-extension task.

METHODS: Thoracic and lumbar flexion-extension data were analyzed to extract the continuous relative phase between each spine subsection. Continuous relative phase data were evaluated using a principal component analysis to identify major sources of variation in spine movement coordination. Unsupervised machine learning (k-means clustering) was used to identify distinct clusters present within the healthy participants sampled. Once distinguished, intersegmental spine kinematics were compared amongst clusters.

RESULTS: The findings of the current work suggest that there are distinct timing strategies that are utilized, within the participants sampled, to control spine flexion-extension movement. These strategies differentiate the sequencing of intersegmental movement and are not discriminable on the basis of simple participant demographic characteristics (ie, age, height, and body mass index), total movement time or range of motion.

CONCLUSIONS: Spatiotemporal spine flexion-extension patterns are not uniform across a population of young healthy individuals.

CLINICAL SIGNIFICANCE: Future work needs to identify whether the motor patterns characterized with this work are driven by distinct neuromuscular activation patterns, and if each given pattern has a varied risk for low back injury.

Keywords: Continuous relative phase; Kinematics; k-means clustering; Machine learning; Movement; Principal component analysis

Introduction

As an anatomically complex series of joints, it is likely that there are a multitude of neuromuscular control options available in the coordination of spine movement. For example, for a given gross spine (ie C7–S1) angular change, it is likely that a variety of sequential local (ie, thoracic-lumbar or intersegmental) movement strategies exist. Although spine motor control has been a heavily researched topic [1], spine kinematics are typically observed through the

FDA Device/Drug Note: Not applicable.

Author disclosures: ***SMB:*** Fellowhip Support: Natural Sciences and Engineering Research Council of Canada (E CAD). ***DPZ:*** Grants: NSERC (D). ***RBG:*** Grants: NSERC (F), Government of Ontario (F). ***SHMB:*** Grants: NSERC (F, paid directly to institution), Ontario Ministry of Research and Innovation (F, outside the submitted work, paid directly to the institution).

* Corresponding author: Department of Human Health and Nutritional Sciences, University of Guelph, Guelph, Ontario, Canada N1G 2W1. Tel.: 519-824-4120, ext. 53651; fax: 519-763-5902.

E-mail address: shmbrown@uoguelph.ca (S.H.M. Brown).

https://doi.org/10.1016/j.spinee.2019.02.002

investigation of specific spine regions (ie, lumbar or thoracic) in isolation [eg 2−5], or through the investigation of a small number of intervertebral motion segments [eg 6−9]. Due to these approaches, the intricacy and resolution of spatiotemporal movement strategies utilized in the coordination of spine movement are largely unknown. Understanding which movement strategies are utilized will allow future research to address both why certain strategies exist, and whether a given motor strategy is associated with spine (dys)function or injury.

Previous work has investigated the spatiotemporal sequencing of spine motion using both cineradiography and optical motion capture approaches. However, the findings are far from unanimous. For example, in the study of the sequencing of lumbar intervertebral flexion-extension motion using cineradiography some studies have reported sequential motion patterns [6] whereas others have reported simultaneous ones [8,9] or a mix of both types [7]. Similarly, in the study of relative thoracic-lumbar flexion-extension timing using optical motion capture, thoracic motion has been shown to both precede and follow lumbar motion [10]. Combined, these findings suggest that different discrete movement strategies may exist in the coordination of multisegment spine kinematics, or that the range of spatiotemporal spine flexion-extension motor strategies is very large.

One way to capture the coordination of complex human movement subsystems is by using relative phase analyses. Continuous relative phase (CRP) measures are particularly well suited to study spatiotemporal patterns in time-evolving systems [11] and are therefore well suited to quantify the patterns of relative rotations between spine regions (ie, thoracic and lumbar) during flexion-extension [12]. Due to this, these measures have been used extensively in the study of sagittal plane spine motion [ie 13−15]. Additionally, unsupervised machine learning techniques, such as *k*-means clustering, can be used to objectively identify systematic trends and groupings present in a sample population [16,17]. By using multisegment spine flexion-extension CRP measures as input parameters for *k*-means, any detectable clustering will be indicative of the spatiotemporal spine flexion-extension strategies utilized within a given sample population. When CRP is calculated using phase-normalized input variables [ie 18−20], such clustering will be independent of natural variations in intersegmental spine kinematics such as those explained by discrete measures of spine range of motion (ROM) or neutral spine posture.

Currently, spine neuromuscular control is an area of heavy research interest [1], with researchers employing a variety of tools to infer spine function and control. Work in this area has identified notable differences in the control of spine movement with low back pain, suggesting that atypical spine motion is a possible risk factor for low back injury [21−23], and possibly an avenue to consider to personalize patient care [24]. However, the current understanding of normal, healthy spine motion is limited. Knowledge of the range of strategies used in the coordination of spine motion in a homogenous sample of healthy individuals will provide a stronger understanding of any particular difference that could be more specifically associated with spine dysfunction and therefore targeted for prehabilitation or rehabilitation approaches. As such, the purpose of the current study was to investigate the natural variability in the spatiotemporal sequencing of spine flexion-extension motion, and to identify if distinct motor strategies exist in a homogenous sample of healthy individuals. It was hypothesized that separate groups would be identifiable in the study dataset, and that when compared statistically, each group would have distinct differences in intersegmental flexion-extension sequencing without any notable variability in demographic (ie, age, height, mass and body mass index [BMI]) or gross spine motor control (ie, movement time, total, thoracic or lumbar ROM) measures.

Methods

Participants

Fifty-one healthy males volunteered to participate in the study. Participant exclusion criteria included the presence of pain within the lumbopelvic region or lower limbs, as well as any diagnosed allergies to adhesives. Each participant completed a general health questionnaire (self-reporting their age, height, and mass) and signed informed consent before data collection. The protocol was approved by the local Research Ethics Board.

Procedure

Participants were required to complete 3 repeated end-range spine flexion-extension movements. Each trial was composed of 2 movements: (1) a flexion movement from a neutral standing position to their perceived maximum spine flexion position, and after a brief hold at this position, (2) extension back to neutral standing. To increase the likelihood that each participant completed the necessary movements by flexing and extending their spine only, each participant's pelvis was strapped to a rigid support to minimize hip flexion and pelvis translation. Furthermore, each participant was instructed to bend forward while only using his spine. This approach emulates previous work investigating isolated spine motion and motor control [eg 25,26]. Each spine flexion task was completed at a comfortable self-selected pace.

Spine flexion kinematics

Participants were outfitted with a grid of 57 reflective kinematic markers (6.5 mm diameter) to track intersegmental spine flexion-extension motion. The middle column (19 markers) was adhered superficial to the palpable spinous processes of the C7−S1 vertebrae in standing. Left and rightward columns were placed 3−5 cm bilaterally at the apex of the left and right paraspinal muscle bellies. Marker

positions were recorded at 120 Hz (OptiTrack, NaturalPoint Inc., Corvalis, USA) and were filtered with a 4th order, zero-lag, low-pass Butterworth filter with an effective cut-off frequency of 2 Hz. All analyses were performed using custom software scripts written in MATLAB (The Mathworks Inc., Natick, MA, USA). The experimental setup is depicted in Fig. 1.

Local coordinate systems (LCS), aligned with the surface of the back, were constructed for each spine level spanning C7–S1 using a method described previously [27]. In brief, each column of markers (left, middle, and right) was linearly extrapolated to provide an additional 3 points at the superior and inferior end of each column of markers. Next, each column of markers was fit with 3D piecewise (5 knots and 6 segments) cubic splines to estimate the curvature of the spine from C7 to S1. At each spine level, a LCS was constructed while referencing each 3D spline. The superior-inferior (SI) vectors of each LCS were tangential to the midline spline. The left and right splines were used to define a curved surface representing the local frontal plane. The anterior-posterior vectors were perpendicular to the SI vectors and normal to the local frontal plane. Last, medial-lateral vectors were perpendicular to the SI and anterior-posterior vectors. This method of constructing LCSs, aligned with the surface of the back, has been shown to be insensitive to marker noise and yields similar lumbar and thoracic angular measures when compared with surface-mounted electromagnetic tracking systems [27]. Total (C7–S1), thoracic (C7–T12), lumbar (T12–S1) and intersegmental (C7–T1 through L5–S1) relative angles were computed between each superior and inferior LCS using a (1) flexion-extension, (2) lateral bend, and (3) axial twist

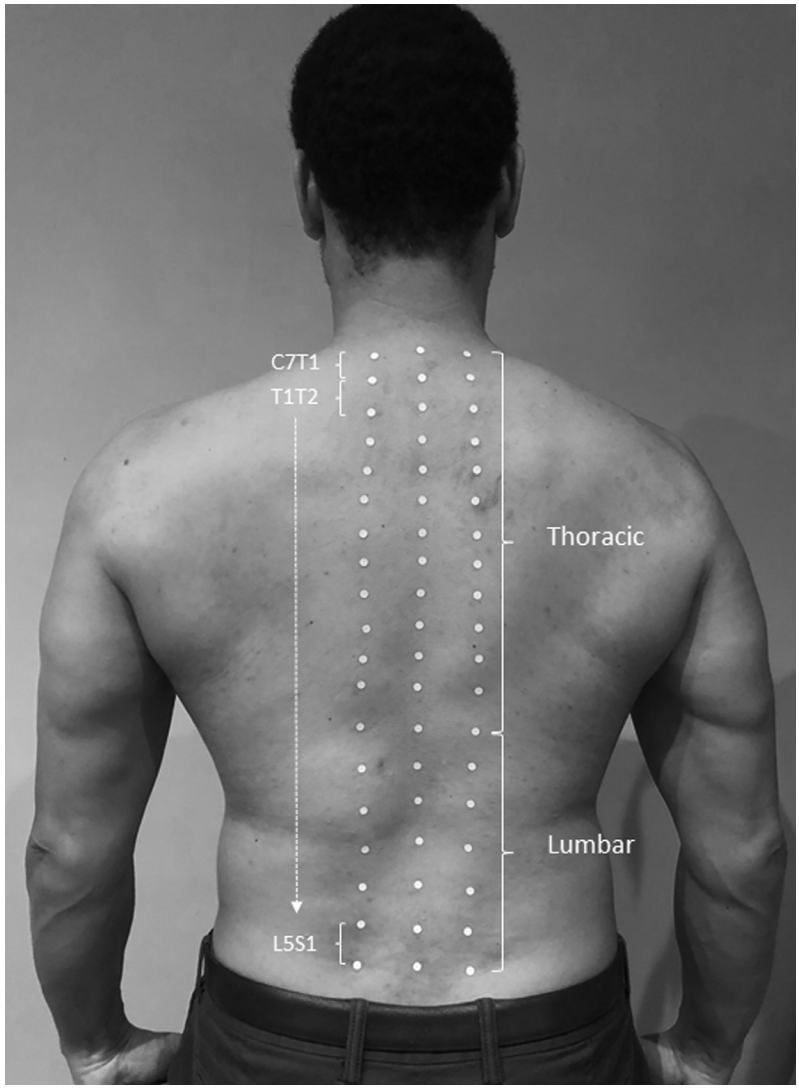

Fig. 1. Depiction of the experimental setup demonstrating the relative locations of each kinematic marker (diameter = 6.5 mm). Markers along the center column were placed superficial to the palpable spinous processes of C7–S1 in a neutral standing posture. Left and right columns were placed 3–5 cm bilaterally, superficial to the left and right paraspinal muscles bellies. Relative angles were computed between local coordinate systems approximating the curvature along the surface of the back to estimate all thoracic, lumbar and intersegmental kinematics.

Cardan sequence. Angular velocities were computed using a 3-point central finite difference approach. As spine motion was restricted to the sagittal plane, only spine flexion-extension angular displacements and velocities were utilized for any further analyses.

Time normalization

Each angular displacement and velocity waveform was time-normalized to 400 frames to account for any variations in trial length. For each flexion-extension trial 3 time points were extracted from the total (C7−S1) angular displacement waveform including movement onset, movement offset, and the instant of peak total spine flexion. All data (ie, thoracic, lumbar, and intersegmental) were time-normalized utilizing these 3 points such that the spine flexion (ie, onset to peak flexion) and spine extension (ie, peak flexion to offset) occurred over 200 frames. By time normalizing in this way, variations in trial length are accounted for, thereby facilitating subsequent ensemble averaging; however, any variations in the spatiotemporal sequencing of spine subsections (ie, thoracic and lumbar) and segments (ie, C7−T1 through L5−S1) are maintained.

Thoracic-lumbar CRP

To dissociate spatiotemporal spine movement strategies, thoracic-lumbar CRP was quantified using methods described previously [eg 12,28]. Although many options for phase-space normalization are available [28], recent work has suggested little influence when comparing phase-space normalization techniques during idealized lifting tasks necessitating spine flexion [12]. Therefore, as is common throughout the literature [eg 18−20,29,30], input waveforms were phase normalized to ensure all angular displacements and velocities ranged between −1 and 1, using the following equation:

$$N(y(t_i)) = 2\left(\frac{y(t_i) - \min(y(t))}{\max(y(t)) - \min(y(t))}\right) - 1, \quad (1)$$

such that N(y(t)) represents the amplitude-normalized signal, and y(t) represents the initial time-varying angular displacement or velocity. The thoracic-lumbar CRP for each flexion-extension movement was then obtained by calculating the 4-quadrant arctangent phase angle from a parametric phase plot (normalized angular displacement vs. normalized angular velocity). The CRP was taken as the lumbar minus thoracic difference between each phase angle at each instant in time over the flexion-extension movement. Using these methods CRP values range in magnitude from −180 to +180 degrees. For the flexion movement positive CRP values indicate that the thoracic motion is preceding lumbar motion. For the extension movement positive CRP values indicate that the lumbar motion is preceding thoracic motion. CRP data were ensemble averaged across each repeated flexion-extension movement for every participant.

Feature reduction: principal component analysis

Principal component analysis (PCA) was performed on the mean thoracic-lumbar CRP angles for all 51 participants to identify the independent factors that account for the majority of variation amongst individuals. PCA of the pooled thoracic-lumbar CRP from multiple participants yields an orthogonal set of waveform features (called loading vectors) and a corresponding set of dimensionless PC-scores for each participant. As a common data reduction technique, PCA reduces the dataset to a linear combination of orthogonal components of variation. To interpret each PC, single component reconstruction was completed to identify biomechanical meaning of each PC with respect to a mean waveform [31]. This step was done to select discrete features that would capture the largest components of variation present within the thoracic-lumbar CRP dataset, and could be used to objectively classify new participants into separate motor subgroups.

k-means clustering

Discrete measures characterizing the 2 major sources of CRP variations were broken into clusters using a *k*-means clustering method. *k*-means clustering aims to partition *n* observations into *k* clusters in which each observation belongs to the cluster with the nearest mean, or centroid, which serves at the prototype for the cluster [16]. Once the location of each centroid is known, future data can be classified by comparing the location of each new data point to the location of each cluster centroid. An inherent risk of the clustering process is the presence of large numbers of samples near the cluster boundaries, which can lead to changes in clustered groups if the analysis is run multiple times. Therefore, despite iterating each individual *k*-means algorithm multiple times with randomly seeded initial centroid locations, convergence to a global optimum is not guaranteed. To accommodate this, the *k*-means clustering algorithm (each with 100 iterations) was repeated 5000 times and the model with the highest number of common iterations (for each given assignment of *k*) was selected. To interpret the strength of each clustering output for multiple assignments of *k,* silhouette coefficients (SCs) were examined with each SC expressing the extent to which clear patterns were distinguished into a given cluster. This measure represents an average of coefficients for each data point indicating the distance of each point to the centroid of a cluster. In general SC values <0.25 suggest the absence of any substantial structure, and those spanning 0.26−0.50, 0.51−0.70 and 0.71−1.00 suggest weak, reasonable, and strong structures, respectively [32]. The clustering structure with the strongest SC and largest number of common model iterations was utilized for all further analyses.

Cluster comparison: spatiotemporal movement strategies

To capture any systematic difference in cluster demographics or gross motor control mean age, height, mass, BMI, movement time, total (C7−S1) ROM, thoracic (C7−T12) ROM, and lumbar (T12−S1) ROM were calculated for each cluster. To identify differences in spatiotemporal movement sequencing, mean amplitude normalized (Eq. 1) flexion-extension angles between adjacent LCSs were computed to be compared within and between each cluster.

Statistical analyses

Discrete measures

Shapiro-Wilk tests were used to assess all discrete dependent variables (ie, age, height, mass, BMI, movement time, total/thoracic/lumbar ROM) for a normal distribution. To assess an effect of cluster, normally distributed data were tested using a one-way analysis of variance (ANOVA); for variables violating normality assumptions, Kruskal-Wallis ANOVAs were used. Post hoc pairwise multiple means comparisons were computed using a Bonferroni correction to protect against an elevated type I error due to multiple comparisons (effective α=0.005 for 10 comparisons). All statistical analyses were performed in MATLAB.

Continuous measures

A statistical parametric mapping (SPM) approach was used to compare all continuous measures (ie, thoracic-lumbar CRP or amplitude normalized intersegmental flexion-extension angles). For all SPM analyses, a scalar output statistic (ie SPM{F}) was calculated for each individual time point. The calculation of SPM{F} indicates the magnitude of difference between mean waveforms, therefore the null hypothesis cannot be accepted or rejected by interpreting these variables alone. To test the null hypothesis (ie, that no significant difference exists) the critical threshold was calculated at which 0.5% of smooth random curves would be expected to traverse (ie, α=0.005). Conceptually an SPM ANOVA is similar to the calculation and interpretation of a scalar ANOVA. If the SPM{F} trajectory crosses the critical threshold (F*) at any time point the null hypothesis is rejected. All SPM analyses were implemented using the open-source spm1d code (v.M.0.4.5, www.spm1d.org) in MATLAB.

For all within-cluster comparisons, a one-way SPM ANOVA was implemented to compare the flexion-extension waveforms from all segments spanning C7−T1 to L5−S1 to identify relative differences in flexion extension timing. For all between-cluster comparisons a one-way SPM ANOVA was again implemented to compare flexion-extension strategies across clusters. Dependent variables included thoracic-lumbar CRP and flexion-extension relative angle waveforms. Post hoc pairwise multiple means comparisons were computed using 2-tailed SPM *t* tests and a Bonferroni correction (effective α=0.005 for 10 comparisons). Unless otherwise stated, all values are presented as means±SD.

Results

Principal component analysis & k-means clustering

The first 2 PCs were found to account for 72.5% of the variability between thoracic-lumbar CRP waveforms (Table 1). Single component reconstruction of each PC outlined that PC1 (45.9% explained variation) was responsible for scaling the CRP waveform during the flexion phase of the movement (Fig. 2A and B). In contrast, PC2 (26.7% explained variation) was responsible for scaling the CRP waveform during the extension phase of the movement (Fig. 2C and D). To accommodate each of these major sources of orthogonal variation (and to allow for the ease of future data classification) the mean CRP was calculated for the flexion (0−200 frames) and extension (200−400 frames) portions of the movement to be used as inputs for *k*-means clustering.

When exploring different assignments of *k*, k=5 demonstrated high clustering structure (SC=0.58) and the highest number of common model iterations (1,783 iterations) and was therefore selected for all further analyses. For any $k\geq6$, single participants were selected for a given cluster thereby inflating estimates of SC, but also dramatically decreasing the number of common number of model iterations (Table 2). Centroid locations for k=5 are depicted in Fig. 3 and are as follows (flexion relative phase, extension relative phase): cluster 1 (C1; 17.3°±9.3°, 13.9°±5.9°), cluster 2 (C2; 6.6°±8.7°, 34.9°±9.6°), cluster 3 (C3; 37.1°±7.4°, 33.8°±5.7°), cluster 4 (C4; −30.6°±15.9°, 18.8°±4.9°), and cluster 5 (C5; 7.5°±16.2°, −16.4°±8.9°).

Discrete measures: between cluster comparisons

No statistically significant differences were observed between clusters for any participant demographic (ie, age, height, mass, and BMI) or gross spine motor control (ie, movement time, total, thoracic, or lumbar ROM) measure at the adjusted critical α=0.005 (Table 3).

Table 1
Variance and cumulative variance in thoracic-lumbar CRP amongst 51 participants explained by the first four principal components (PCs). PC1 and PC2 (bolded) were used in the selection of a discrete measure (ie mean flexion and mean extension CRP) to differentiate CRP waveforms using *k*-means clustering.

PC	Explained Variance (%)	Cumulative Variance (%)
1	**45.9**	**45.9**
2	**26.7**	**72.6**
3	12.9	85.5
4	5.5	91.0

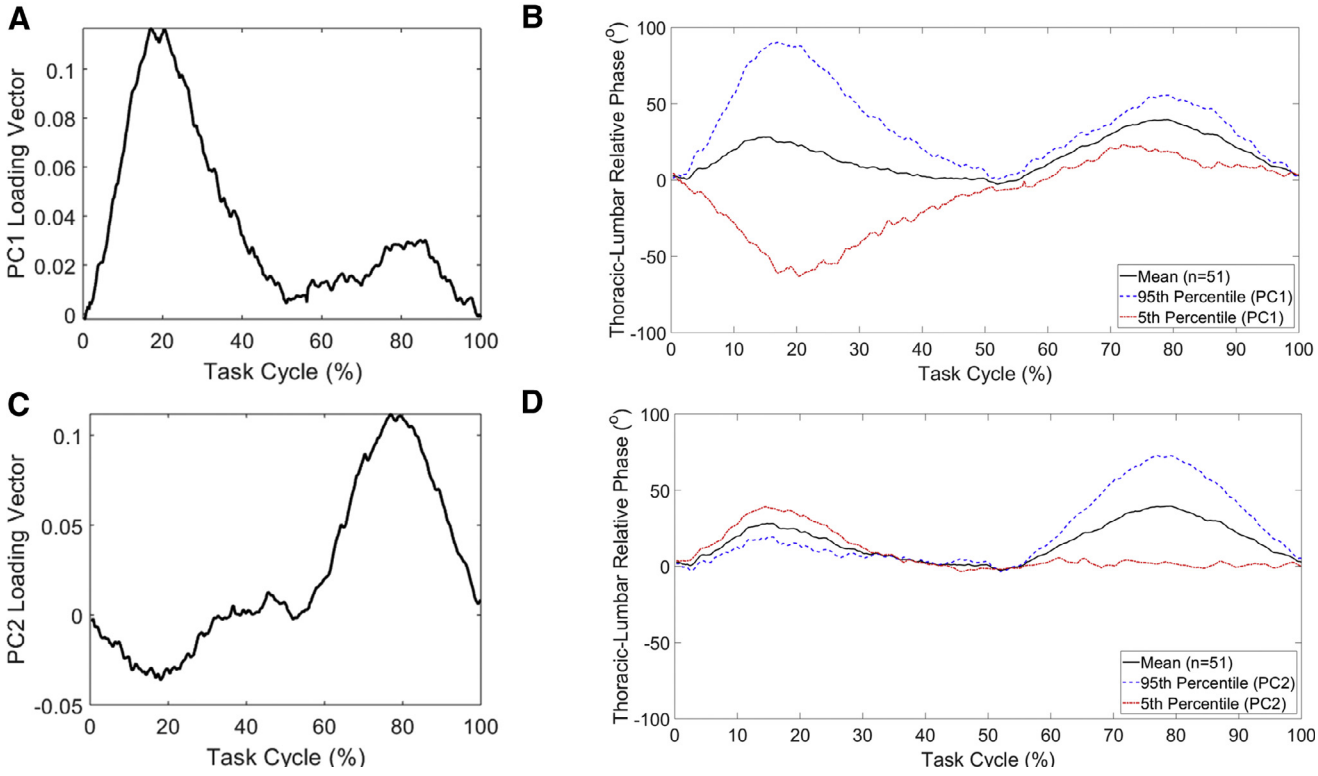

Fig. 2. Depiction of the first 2 principal components (PCs) which explain the largest variations in thoracic-lumbar continuous relative phase. (A) The PC1 loading vector demonstrating the largest influence during the flexion portion of the spine flexion-extension movement. (B) Single component reconstruction of PC1 demonstrating the 5th and 95th percentile PC1 scores relative to the mean (N=51). (C) The PC2 loading vector demonstrating the largest influence during the extension portion of the spine flexion-extension movement. (D) Single component reconstruction of PC2 demonstrating the 5th and 95th percentile PC2 scores relative to the mean (N=51).

Thoracic-lumbar CRP

A significant main effect was observed (Fig. 4), suggesting that the thoracic-lumbar CRP of clusters 1−5 significantly differed during the spine flexion (7%−38% of task cycle) and extension (62%−95% of task cycle) movements (p<.001). Specifically, the C1 thoracic-lumbar CRP was significantly different from C3 (16%−23% of task cycle; p<.001) and C4 (10%−26% of task cycle; p<.001) during spine flexion, and significantly different from C2 (68%−88% of task cycle; p<.001) and C5 (62%−88% of task cycle; p<.001) during spine extension. Additionally, the C2 thoracic-lumbar CRP was significantly different from C3 (10%− 26% of task cycle; p<.001) and C4 (15%−22% of task cycle; p<.001) during spine flexion, and from C5 (62%−89% of task cycle; p<.001) during spine extension. Further, the C3 thoracic-lumbar CRP was significantly different from C4 (8%− 27% of task cycle; p<.001) and C5 (17%−19% of task cycle; p=.002) during spine flexion, and from C5 (62%−92% of task cycle; p<.001) during spine extension. Finally, the C4 thoracic-lumbar CRP was significantly different from C5 during a small subset of the extension movement (68%−70% of task cycle; p<.001).

Table 2
The relative strength of each k-means clustering output when separated into *k* clusters assessed using each model's mean silhouette coefficient (SC) and the highest number of common model iterations (out of 5000 total). *k*=5 (bolded) was selected as the optimal value and used in subsequent analyses. Crosses indicate models where individual participants were identified for a given cluster.

k	SC	Iterations (/5000)
2	0.5399	1656
3	0.5891	498
4	0.5085	770
5	**0.5846**	**1783**
6+	0.5929	483
7+	0.6142	77

Intersegmental kinematics

Within each cluster, clear differences in the sequencing of spine flexion and extension motion were observed (Fig. 5) with a significant main effect of spine level (ie, C7−T1 through L5−S1) existing within each cluster at distinct sections of the flexion-extension movement. For C1, a significant main effect was observed throughout much of the flexion-extension movement (0%−68% and 77%−100% of task cycle; p<.001). During spine flexion,

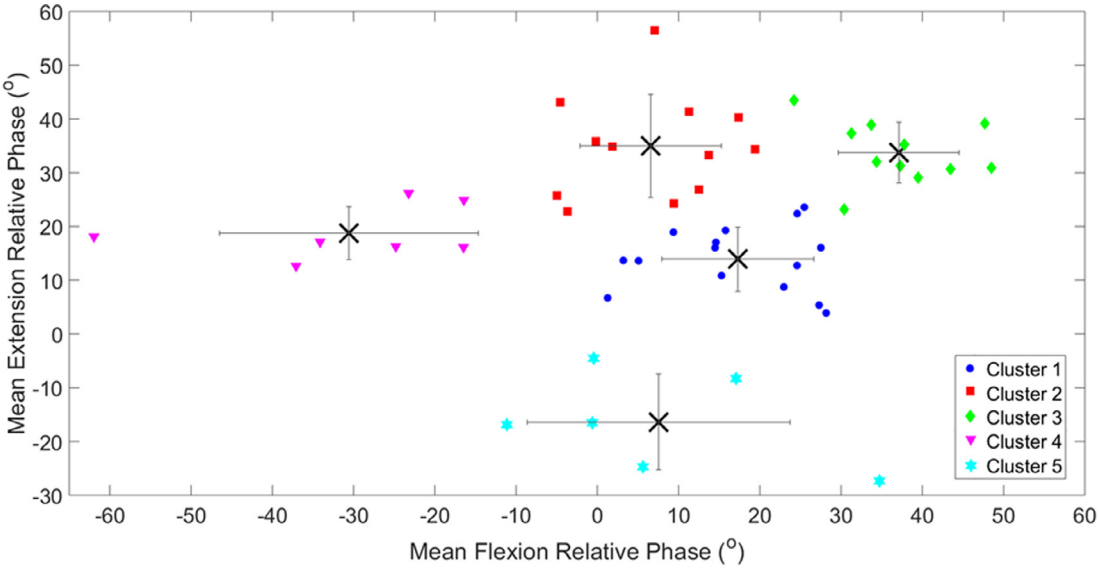

Fig. 3. A 2D scatterplot demonstrating the clusters (k=5) characterized by the k-means classification method. Each cluster centroid is denoted by an x-symbol. Errors bars depict standard deviations along each dimension (ie mean flexion relative phase or mean extension relative phase).

lower thoracic segments appeared to lead upper thoracic and lumbar segments. During extension, most segments appeared to move in synchrony. For C2 and C3, a significant main effect was observed throughout the entirety of the flexion-extension movement (0%−100% of task cycle; p<.001). For C2, the flexion strategy appeared to be similar to that of C1 (ie, lower thoracic segments leading upper thoracic and lumbar); however, during the extension movement a bottom-up strategy existed whereby motion initiated through lumbar segments and progressed to upper-thoracic ones. For C3, thoracic segments were observed to lead lumbar segments during spine flexion, and trail lumbar segments during spine extension. For C4, a significant main effect was observed during both the flexion (16%−43% of task cycle; p<.001) and extension (79%−100% of task cycle; p<.001) movements. During flexion, lumbar and lower thoracic segments appeared to initiate the movement whereas the upper thoracic segments appeared to lag behind. During extension, lower lumbar segments appeared to move first, followed by all thoracic segments. For C5 a significant main effect was observed during extension (63%−77% of task cycle; p<.001) movement. The notable trend within C5 during extension was that the upper thoracic segments were observed to lead lower thoracic and lumbar ones.

Amongst clusters, differences in intersegmental kinematics existed primarily within upper thoracic and lower lumbar segments (Fig. 6). Significant main effects were found during the flexion movement for C7T1 (17%−41% of task cycle; p<.001), T1T2 (16%−40%; p<.001), T2T3 (16%−40%; p<.001), T3T4 (13%−40%; p<.001), T4T5 (9%−37%; p<.001), L2L3 (9%−25%; p<.001), L3L4 (4%−24%; p<.001), L4L5 (4%−22%; p<.001), and L5S1 (6%−23%; p<.001). Additionally, significant main effects were also observed during the extension movement for C7T1 (63%−80% of task cycle; p<.001). T1T2 (61%−79%; p<.001), T2T3 (60%−79%; p<.001), T3T4 (61%−85%; p<.001), T4T5 (61%−89%; p<.001), L3L4 (78%−89%; p<.001), L4L5 (74%−87%; p<.001), and L5S1 (71%−87%; p<.001). Post-hoc analyses (Table 4) indicate a general trend such that, during flexion, C1 and C3 present with earlier flexion patterns in upper thoracic segments than C2, C4, and C5. Additionally, C1 and C3 demonstrate delayed flexion

Table 3
Mean±standard deviation participant demographic and gross spine motor control measures. Main effect p values are italicized, with crosses indicating the results of a Kruskal-Wallis nonparametric ANOVA

Group	Age (years)	Height (m)	Mass (kg)	BMI (kg/m^2)	Movement Time (s)	Total ROM (°)	Thoracic ROM (°)	Lumbar ROM (°)
All *(n = 51)*	24.0 ± 3.3	1.80 ± 0.07	80.4±11.0	24.8±3.5	14.0±5.8	82.9±13.0	33.6±10.3	51.1±10.7
Cluster 1 *(n = 15)*	23.0 ± 2.9	1.82 ± 0.08	81.5±12.5	24.6±3.4	12.3±3.3	85.2±10.5	35.3±9.1	51.1±9.2
Cluster 2 *(n =12)*	26.4 ± 3.6	1.81 ± 0.06	81.7±6.5	24.9±1.6	16.0±5.6	88.1±16.8	37.1±10.5	52.7±13.0
Cluster 3 *(n = 11)*	22.9 ± 3.1	1.80 ± 0.06	82.5±14.0	25.5±4.9	15.6±9.0	83.0±7.1	35.2±6.6	50.6±5.5
Cluster 4 *(n = 7)*	23.9 ± 2.5	1.76 ± 0.06	74.7±7.8	24.2±2.9	14.3±4.8	78.0±12.1	26.7±9.1	53.4±12.4
Cluster 5 *(n = 6)*	24.0 ± 3.2	1.79 ± 0.09	77.9±11.7	24.4±4.8	10.7±2.4	72.0±15.4	27.9±16.1	46.3±15.9
p-value	*.0354*$^+$	*.5016*	*.5926*	*.9409*	*.1242*$^+$	*.1046*	*.1294*	*.7823*

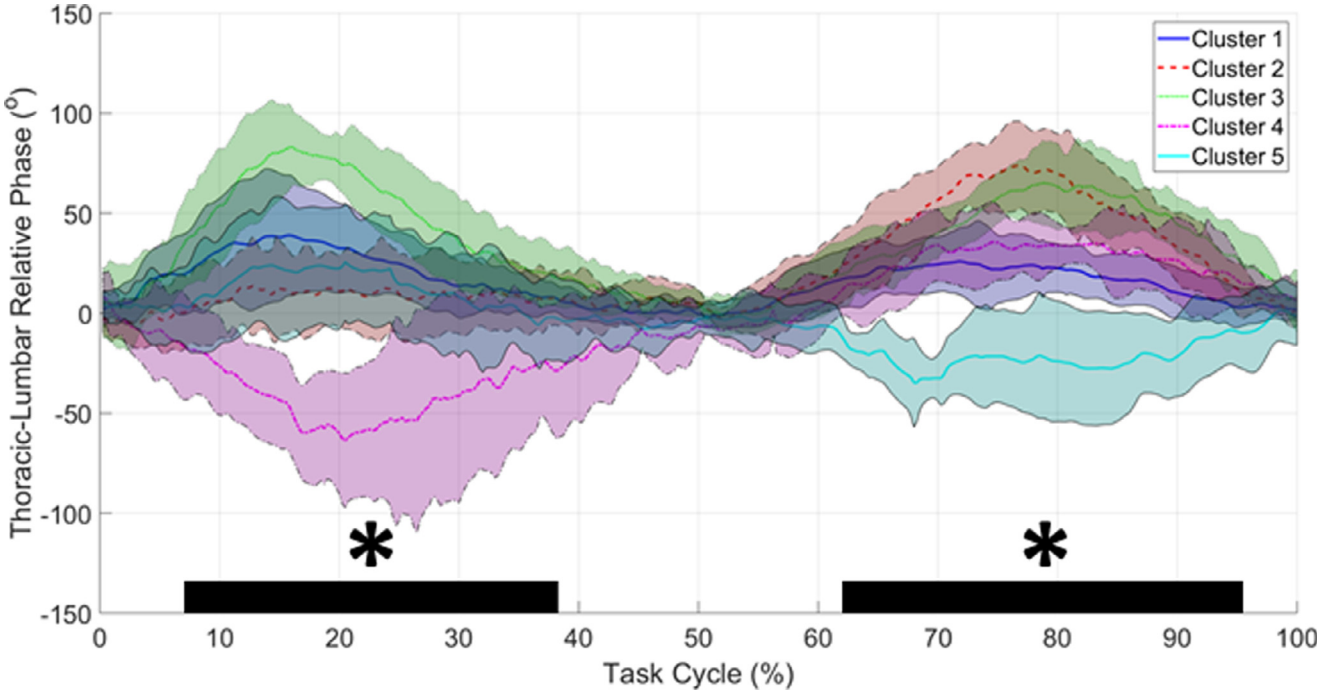

Fig. 4. Mean (±SD) thoracic-lumbar continuous relative phase for each *k*-means cluster. Asterisks denote significant SPM main effects between clusters for a given time band (p<.001). Please note that for the flexion movement positive CRP values indicate that the thoracic motion is preceding lumbar motion. For the extension movement positive CRP values indicate that the lumbar motion is preceding thoracic motion.

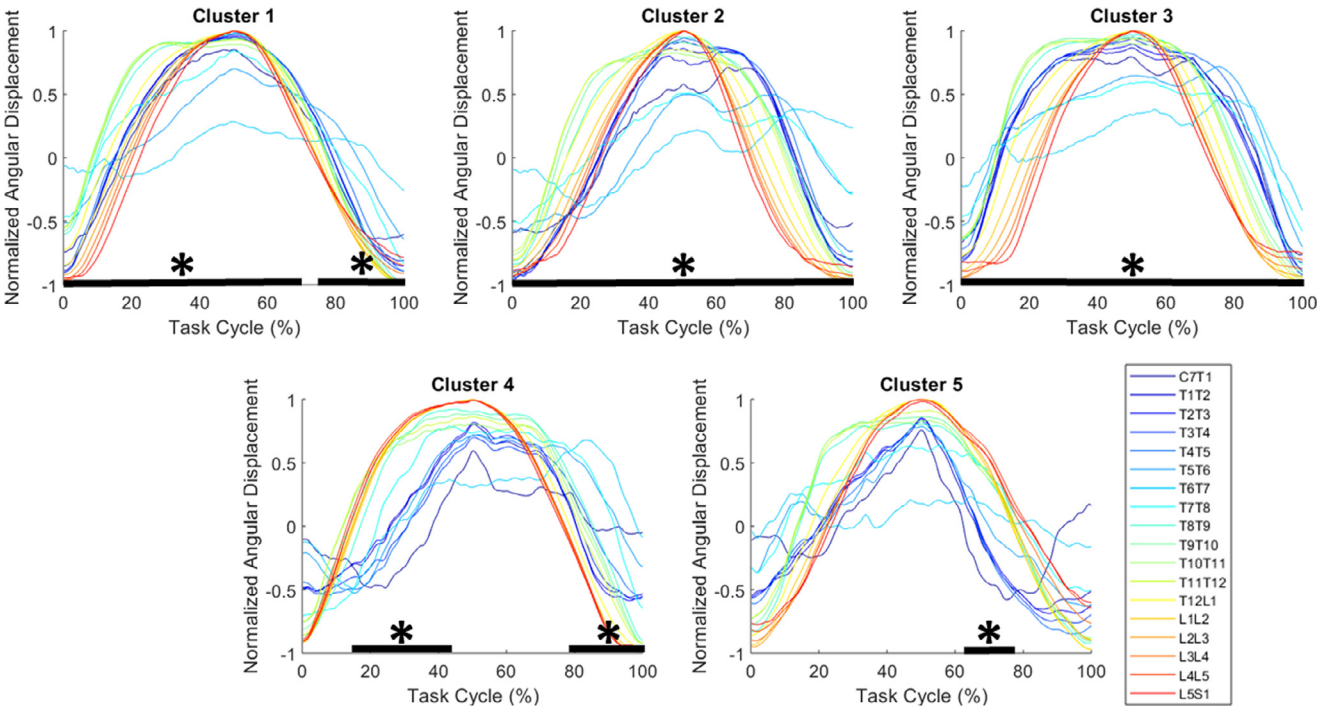

Fig. 5. Mean spatiotemporal flexion-extension strategies between adjacent LCS within each *k*-means cluster. Asterisks denote significant SPM main effects amongst intersegmental levels for a given time band (p<.001).

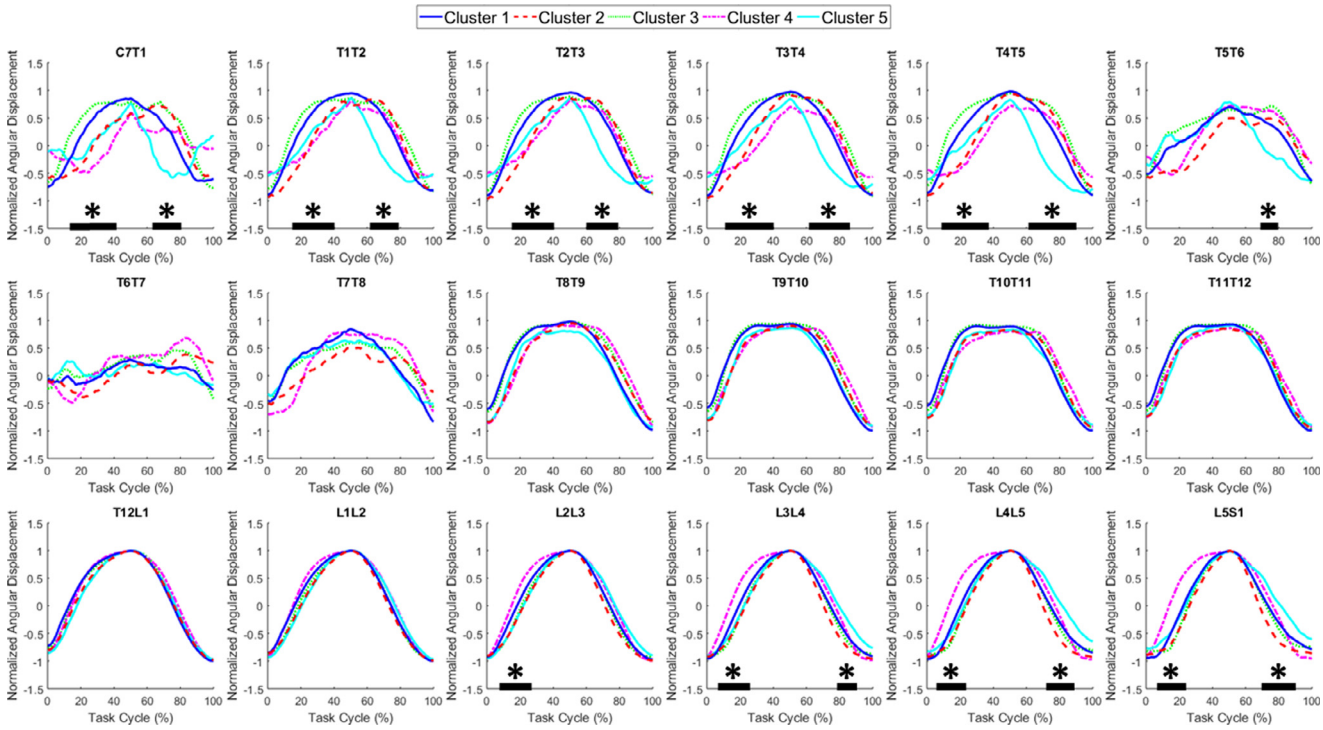

Fig. 6. Comparison of mean spatiotemporal flexion-extension strategies amongst *k*-means clusters. Asterisks denote significant SPM main effects amongst clusters for a given time band (p<.001).

Table 4
Pairwise post-hoc intersegmental comparisons amongst *k*-means clusters (C1–C5). Differences during flexion are located to the left of the main diagonal. Differences during extension are located to the right of the main diagonal. All significant differences (p≤.005) for each intersegmental level are bolded, with the timing (% of task cycle) of each regional difference in brackets.

	C1	C2	C3	C4	C5
C1	–	All p≥.005	All p≥.005	All p≥.005	**T1T2 (63–74%)** **T2T3 (63–73%)** **T3T4 (63–74%)** **T4T5 (63–77%)**
C2	All p≥.005	–	All p≥.005	All ≥.005	**C7T1 (66–78%)** **T1T2 (63–78%)** **T2T3 (63–78%)** **T3T4 (63–81%)** **T4T5 (63–84%)** **L3L4 (76–81%)** **L5S1 (76–79%)**
C3	All p≥.005	**C7T1 (16–30%)** **T1T2 (14–27%)** **T2T3 (13–27%)** **T3T4 (6–28%)** **T4T5 (6–28%)**	–	All p≥.005	**C7T1 (64–75%)** **T1T2 (64–73%)** **T2T3 (63–73%)** **T3T4 (63–76%)** **T4T5 (63–87%)** **T5T6 (71–79%)**
C4	**C7T1 (29–37%)** **T1T2 (34–39%)** **T2T3 (33–39%)** **L4L5 (2–11%)** **L5S1 (3–14%)**	All p≥.005	**C7T1 (21–36%)** **T2T3 (32–36%)** **T3T4 (18–31%)** **T4T5 (17–27%)** **L2L3 (10–18%)** **L3L4 (5–21%)** **L4L5 (8–20%)** **L5S1 (8–20%)**	–	All p≥.005
C5	All p≥.005	All p≥.005	**C7T1 (24–30%)** **T1T2 (25–33%)** **T2T3 (31–33%)** **T3T4 (30–35%)**	All p≥.005	–

patterns in lower lumbar segments relative to C4. During extension, C5 tends to have earlier extension in upper thoracic segments relative to C1, C2, and C3. Additionally, C5 demonstrated a delayed extension strategy in L5S1 relative to C2.

Discussion

The purpose of the current work was to investigate the range of multisegment movement timing strategies utilized in the coordination of spine flexion-extension. It was hypothesized that separate groups would be identifiable within the study dataset, and that while these groups would present with distinct spatiotemporal spine movement strategies they would not be discriminable on the basis of participant demographic characteristics or gross spine motor control measures. Overall, the findings support these hypotheses.

Upon investigating the largest components of variation in thoracic-lumbar CRP (Table 1 and Fig. 2), it was clear that a range of motor strategies existed during the completion of spine flexion (ie PC1) and spine extension (ie PC2). To capture these large components of variation, mean flexion and extension CRP were used as input features for *k*-means clustering. The optimal value for *k* was determined to be *k*=5 which presented with both a high SC (0.58) and number (1,783) of model iterations (Table 2 and Fig. 3). Although no significant differences were observed between *k*-means clusters regarding participant demographics or gross spine motor control (Table 3), each cluster had significantly different thoracic-lumbar CRP waveforms (Fig. 4). Furthermore, each cluster presented with distinct spatiotemporal intersegmental flexion-extension strategies (Fig. 5) with the largest between cluster differences occurring in the timing of upper thoracic (ie, C7–T1 through T5–T6) and lower lumbar (ie, L2–L3 through L5–S1) motion segments (Fig. 6 and Table 4).

The findings of the current work add to those within the literature in a variety of ways. First, the current findings suggest that thoracic-lumbar CRP measures have the capability to differentiate distinct spatiotemporal sequencing strategies during spine flexion-extension. This expands on the utility of CRP as a measure to examine the coordination between absolute segment rotations of the thorax and pelvis [33,34], or relative rotations between the lumbar spine and lower limb joints [13,14,35]. Second, the results from the current work agree with previous studies that have investigated the spatiotemporal sequencing of spine motion. Previous research studies have suggested lumbar intervertebral flexion-extension movement to be sequential [6], simultaneous [8,9] as well as a mix of both [7]. Similarly, in the study of relative thoracic-lumbar flexion-extension timing, thoracic motion has been shown to both precede and follow lumbar motion [10]. Based on the current results, it is clear that each of these spine motor strategies does exist. For example, when comparing C3 and C4 clusters during spine flexion the current findings suggest that thoracic motion may both precede (C3) or follow (C4) lumbar motion; similarly, lumbar motion can be both sequential (C3) or simultaneous (C4). These phenomena also exist during spine extension. Third, the current results suggest that a wide range of motor strategies exist, even within a homogenous sample of young healthy adult males with comparable functional capacities (ie, ROM). This finding is relevant, as although functional evaluation of the spine has the potential to support the identification of spine pathologies, it is important to first ascertain an in-depth understanding of normal kinematics.

Although the results of the current work demonstrate the existence of distinct spine spatiotemporal flexion-extension strategies, it is currently unclear why the given set of strategies exist, or whether a given motor strategy is associated with spine (dys)function or injury. Each of these questions has potential avenues for future study. To investigate the cause of the specific motor strategies observed here, regional muscle activations may be examined using high density surface electromyography [ie 36,37]. Such an approach would link the observed motor strategies with regional neuromuscular activation patterns along segmented (ie, innervations and lines of action) muscles such as the erector spinae or multifidus. Further, to investigate the relative risk for injury across motor strategies, the clusters identified here could be tracked longitudinally and/or investigated using a biomechanical modeling approach to estimate biomechanical risk factors such as spine loading [ie 38,39], or mechanical stability [ie 40].

The workflow developed and utilized within the current study serves as a proof of principle, demonstrating that separate spine movement patterns can be distinguished using thoracic-lumbar CRP and unsupervised machine learning approaches such as k-means clustering. Machine learning applications in biomechanics have received considerable attention recently [17]; however, the use these approaches rely on several mathematical postulates such as the selection of an input feature matrix (X), or number of clusters (k) for *k*-means. For the current approach, CRP measures were used as input features due to their strong track record of distinguishing spatiotemporal movement patterns in spine biomechanics when assessing the effects of back pain [14], fatigue [15], age [34], and lifting technique [41]. Although these measures have shown promising findings here, it is possible that different combinations of input features will yield different clustering results, potentially capturing different phenomena. Further, there has been a considerable amount of debate surrounding phase space normalization for CRP analyses, with some authors using only time-normalization [42], others using the same phase space normalization procedures used within the current work [eg 18–20,29,30], and others suggesting the use of a Hilbert transform to remove potential frequency artefacts [28,43]. As recent findings have suggested against a superior methodological approach to discriminate between spine

flexion-extension style movements [12], we utilized the phase space normalization approach (Eq. 1), as this was the most common approach used throughout the research literature. Additionally, we utilized PCA as a feature reduction method and as a tool to include features capturing the largest components of interindividual variability within the dataset (eg, mean flexion and extension thoracic-lumbar CRP). Finally, since the number of spatiotemporal sequencing strategies in the coordination of spine flexion-extension is unknown, no *a priori* selection of k could be made. To accommodate this uncertainty, we assessed the clustering structure with different assignments of k and selected the value objectively on the basis of each model's SC, number of model iterations, and distribution of the data throughout each cluster (eg, avoiding the occurrence of a single participant being selected as the centroid for any given cluster). Although we believe that each step of the current analysis is supported by existing research literature, future research will need to refine unsupervised machine learning approaches for applications in spine biomechanics.

There are some limitations to consider when interpreting the findings of this work. The first limitation concerns the modest sample size (N=51) used in the current analyses. Although this study identifies 5 specific clusters of spine movement with reasonable clustering structure (SC=0.58), and is within the range of sample sizes reported within the literature [17], it is possible that, on the population level, the clustering of participants in this way may not occur (ie, different clusters may be present, or the data may be continuous). A second limitation to consider is that, although the clustering outputs identified here are supported by previous works [eg 6–10], they could not be completely validated, and are therefore limited to the selected analyses and analyzed movements. To validate the current findings, each participant's movement strategy would need to be identified *a priori*. As this information was unknown, the current methods for distinguishing separate motor strategies are unsupervised (ie, are not based on any known validated data labels). Because of this, the current analysis identifies commonalities in the dataset, and clusters the data based on self-similarities between data points. A strength of this approach is the ability to highlight new, otherwise unforeseen trends within a dataset such as the variable spatiotemporal strategies to flex/extend the spine, even across a homogenous sample of healthy males. This is something that may be overlooked during the mean comparison of a healthy functioning group to patient groups such as those with lower back pain. The third limitation concerns the use of a surface kinematic model to estimate the relative position and orientation of the bony vertebrae. Due to the nature of skin based-kinematic tracking, the locations and orientation of each vertebrae during the dynamic spine flexion-extension tasks can only be approximated (ie, due to associated soft tissue artefacts). However, previous work has suggested that surface markers can approximate vertebral motion when the motion is in the sagittal plane [44], and the kinematic model used here has been shown to be robust to noise during spine flexion [27].

Conclusions

Even within a homogenous group of healthy young males, spatiotemporal spine flexion-extension patterns are not uniform. Five distinct motor strategies were identified using thoracic-lumbar CRP and k-means clustering. During flexion, some clusters tended to initiate flexion with lower thoracic segments (i.e. C1, C2 and C5), whereas others initiated flexion with upper thoracic (C3) or lower lumbar (C4) segments. During extension some clusters initiated the movement through lumbar segments (ie, C2, C3, and C4) whereas others initiated the movement with upper thoracic segments (C5) or adopted a more simultaneous movement strategy (C1). The largest between cluster differences in the timing of movement occurred in upper thoracic (ie, C7–T1 through T5–T6) and lower lumbar (ie, L2–L3 through L5–S1) regions (Fig. 6 and Table 4). Whether the spatiotemporal movement strategies observed here are dictated by specific regional muscular activation strategies or result in altered injury risk are potential avenues for future study.

Acknowledgment

This work was funded by grants from the Natural Sciences and Engineering Research Council (NSERC) 402407-2013 of Canada.

References

[1] van Dieën JH, Reeves NP, Kawchuck G, van Dillen LR, Hodges PW. Motor control changes in low-back pain: divergence in presentations and mechanisms. J Orthop Sports Phys Ther 2018. epub ahead of print https://doi.org/10.2519/jospt.2019.7917.

[2] Sullivan MS, Dickenson CE, Troup JDG. The influence of age and gender on lumbar spine sagittal plane range of motion: a study of 1126 healthy subjects. Spine 1994;19:682–6.

[3] Swinkels A, Dolan P. Regional assessment of joint position sense in the spine. Spine 1998;23:590–7.

[4] List R, Gülay T, Stoop M, Lorenzetti S. Kinematics of the trunk and the lower extremities during restricted and unrestricted squats. J Strength Cond Res 2013;27:1529–38 https://doi.org/10.1519/JSC.0b013e3182736034.

[5] Howarth SJ. Comparison of 2 methods of measuring spine angular kinematics during dynamic flexion movements: skin-mounted markers compared to markers affixed to rigid bodies. J Manipulative Physiol Ther 2014;37:688–95 https://doi.org/10.1016/j.jmpt.2014.10.006.

[6] Kanayama M, Abumi K, Kaneda K, Tadano S, Ukai T. Phase lag of the intersegmental motion in flexion-extension of the lumbar and lumbosacral spine: an in vivo study. Spine 1996;21:1416–22.

[7] Okawa A, Shinomiya K, Komori H, Muneta T, Arai Y, Nakai O. Dynamic motion study of the whole lumbar spine by videofluoroscopy. Spine 1998;23:1743–9.

[8] Lee S-W, Wong KWN, Chan M-K, Yeung H-M, Chiu JLF, Leong JCY. Development and validation of a new technique for assessing lumbar spine motion. Spine 2002;27:E215–E20.

[9] Wong KWN, Leong JCY, Chan M-K, Lu WW. The flexion-extension profile of lumbar spine in 100 healthy volunteers. Spine 2004;29:1636–41 https://doi.org/10.1097/01.BRS.0000132320.39297.6C.

[10] Ignasiak D, Rüeger A, Ferguson SJ. Multi-segmental thoracic spine kinematics measured dynamically in the young and elderly during flexion. Hum Mov Sci 2017;54:230–9 https://doi.org/10.1016/j.humov.2017.05.011.
[11] Hamill J, Palmer C, van Emmerik REA. Coordinative variability and overuse injury. Sport Med Arthrosc Rehabil Ther Technol 2012;4:45 https://doi.org/10.1186/1758-2555-4-45.
[12] Zehr JD, Howarth SJ, Beach TAC. Using relative phase analysis and vector coding to quantify pelvis-thorax coordination during lifting – a methodological investigation. J Electromyogr Kinesiol 2018;39:104–13 https://doi.org/10.1016/j.jelekin.2018.02.004.
[13] van Die.n JH, Toussaint HM, Maurice C, Mientjes M. Fatigue-related changes in the coordination of lifting and their effects on low back load. J Mot Behav 1996;28:304–14 https://doi.org/10.1080/00222895.1996.10544600.
[14] Commissaris DA, Nilsson-Wikmar LB, van Dieën JH, Hirschfeld H. Joint coordination during whole body lifting in women with low back pain after pregnancy. Arch Phys Med Rehabil 2002;83:1279–89 https://doi.org/10.1053/apmr.2002.33641.
[15] Hu B, Ning X. The influence of lumbar extensor muscle fatigue on lumbar-pelvic coordination during weightlifting. Ergonomics 2015;58:1424–32 https://doi.org/10.1080/00140139.2015.1005173.
[16] Jain AK, Murty MN, Flynn PJ. Data clustering: a review. ACM Comput Surv 1999;31:264–323 https://doi.org/10.1145/331499.331504.
[17] Halilaj E, Rajagopal A, Fiterau M, Hicks JL, Hastie TJ, Delp SL. Machine learning in human movement biomechanics: best practices, common pitfalls, and new opportunities. J Biomech 2018;81:1–11 https://doi.org/10.1016/j.jbiomech.2018.09.009.
[18] Van Emmerik REA, Wagenaar RC. Effects of walking velocity on relative phase dynamics of the trunk in human walking. J Biomech 1996;29:1175–84 https://doi.org/10.1016/0021-9290(95)00128-X.
[19] Selles RW, Wagenaar RC, Smit TH, Wuisman PIJM. Disorders in trunk rotation during walking in patients with low back pain: a dynamical systems approach. Clin Biomech 2001;16:175–81 https://doi.org/10.1016/S0268-0033(00)00080-2.
[20] Lamoth CJC, Beek PJ, Meijer OG. Pelvis-thorax coordination in the transverse plane during gait. Gait Posture 2002;16:101–14 https://doi.org/10.1016/S0966-6362(01)00146-1.
[21] Hodges PW. Pain and motor control: from the laboratory to rehabilitation. J Electromyogr Kinesiol 2011;21:220–8 https://doi.org/10.1016/j.jelekin.2011.01.002.
[22] Hodges PW, Moseley GL. Pain and motor control of the lumbopelvic region: effect and possible mechanisms. J Electromyogr Kinesiol 2003;13:361–70 https://doi.org/10.1016/S1050-6411(03)00042-7.
[23] O'Sullivan P. Diagnosis and classification of chronic low back pain disorders: maladaptive movement and motor control impairments as underlying mechanism. Man Ther 2005;10:242–55 https://doi.org/10.1016/j.math.2005.07.001.
[24] van Dieën JH, Reeves NP, Kawchuck G, van Dillen LR, Hodges PW. Analysis of motor control in low back pain patients: a key to personalized care? J Orthop Sports Phys Ther 2018. epub ahead of print https://doi.org/10.2519/jospt.2019.7916.
[25] Granata K, England S. Stability of dynamic trunk movement. Spine 2006;31:e271–e6 https://doi.org/10.1097/01.brs.0000216445.28943.d1.
[26] Graham RB, Brown SHM. Local dynamic stability of spine muscle activation and stiffness patterns during repetitive lifting. J Biomech Eng 2014;136:121006 https://doi.org/10.1115/1.4028818.
[27] Zwambag DP, Beaudette SM, Gregory DE, Brown SHM. Development of a novel technique to record 3D intersegmental angular kinematics during dynamic spine movements. Ann Biomech Eng 2018;46:298–309 https://doi.org/10.1007/s10439-017-1970-x.
[28] Lamb PF, Stockl M. On the use of continuous relative phase: review of current approaches and outline for a new standard. Clin Biomech 2014;29:484–93 https://doi.org/10.1016/j.clinbiomech.2014.03.008.
[29] Haddad JM, van Emmerik REA, Wheat JS, Hamill J, Snapp-Childs W. Relative phase coordination analysis in the assessment of dynamic gait symmetry. J Appl Biomech 2010;26:109–13 https://doi.org/10.1123/jab.26.1.109.
[30] Figueiredo P, Deifert L, Vilas-Boas JP, Fernandes RJ. Individual profiles of spatio-temporal coordination in high intensity swimming. Hum Mov Sci 2012;31:1200–12 https://doi.org/10.1016/j.humov.2012.01.006.
[31] Brandon SCE, Graham RB, Almosnino S, Sadler EM, Stevenson JM, Deluzio KJ. Interpreting principal components in biomechanics: representative extremes and single component reconstruction. J Electromyogr Kinesiol 2013;23:1304–10 https://doi.org/10.1016/j.jelekin.2013.09.010.
[32] Struyf A, Hubert M, Rousseeuw PJ. Clustering in an object-oriented environment. J Stat Softw 1996;1:1–30 http://dx.doi.org/10.18637/jss.v001.i04.
[33] Shojaei I, Vazirian M, Salt EG, van Dillen LR, Bazrgari B. Timing and magnitude of lumbar spine contribution to trunk forward bending and backward return in patients with acute low back pain. J Biomech 2017;53:71–7 https://doi.org/10.1016/j.jbiomech.2016.12.039.
[34] Vazirian M, Shojaei I, Bazrgari B. Age-related differences in the timing aspect of lumbopelvic rhythm during trunk motion in the sagittal plane. Hum Mov Sci 2017;51:1–8 https://doi.org/10.1016/j.humov.2016.10.010.
[35] Scholz JP. Organizational principles for the coordination of lifting. Hum Mov Sci 1993;12:537–76 https://doi.org/10.1016/0167-9457(93)90004-9.
[36] Abboud J, Nougarou F, Lardon A, Dugas C, Descarreaux M. Influence of lumbar muscle fatigue on trunk adaptations during sudden external perturbations. Front Hum Neurosci 2016;10:576 https://doi.org/10.3389/fnhum.2016.00576.
[37] Afsharipour B, Petracca F, Gasparini M, Merletti R. Spatial distribution of surface EMG on trapezius and lumbar muscles of violin and cello players in single note playing. J Electromyogr Kinesiol 2016;31:144–53 https://doi.org/10.1016/j.jelekin.2016.10.003.
[38] Marras WS, Sommerich CM. A three-dimensional motion model of loads on the lumbar spine: I. Model structure. Hum Factors 1991;33:123–37 https://doi.org/10.1177/001872089103300201.
[39] Christophy M, Faruk Senan NA, Lotz JC, O'Reilly OM. A musculoskeletal model of the lumbar spine. Biomech Model Mechanobiol 2012;11:19–34 https://doi.org/10.1007/s10237-011-0290-6.
[40] Cholewicki J, McGill SM. Mechanical stability of the *in vivo* lumbar spine: implications for injury and chronic low back pain. Clin Biomech 1996;11:1–15 https://doi.org/10.1016/0268-0033(95)00035-6.
[41] Burgess-Limerick R, Abernathy B, Neal RJ. Relative phase quantifies inter-joint coordination. J Biomech 1993;26:91–4 https://doi.org/10.1016/0021-9290(93)90617-N.
[42] Silfies SP, Bhattacharya A, Biely S, Smith SS, Giszter S. Trunk control during standing reach: a dynamical system analysis of movement strategies in patients with mechanical low back pain. Gait Posture 2009;29:370–6 https://doi.org/10.1016/j.gaitpost.2008.10.053.
[43] Lamoth CJC, Daffertshofer A, Huys R, Beek PJ. Steady and transient coordination structures of walking and running. Hum Mov Sci 2009;28:371–86 https://doi.org/10.1016/j.humov.2008.10.001.
[44] Zemp R, List R, Gülay T, Elsig JP, Naxera J, Taylor WR, et al. Soft tissue artefacts of the human back: comparison of the sagittal curvature of the spine measured using skin markers and open upright MRI. PLoS One 2014;9:e95426 https://doi.org/10.1371/journal.pone.0095426.